On Geometric Correction Method of BJ-1 Panchromatic Image Covering Kingdom of Lesotho

Shunxi LIU[1*], Zhongwu WANG[1], Wei HAO[2], Rongbin WANG[1]

1. China Land Surveying & Planning Institute, Beijing 100035, China; 2. Gansu Land Resource Survey and Planning Institute, Lanzhou 730000, China

Abstract The purpose is to find a suitable geometric correction method of BJ-1 panchromatic image covering Kingdom of Lesotho. The methods are carrying out two geo-correction experiments based on the push-broom model and the projective transform model for BJ-1 small satellite real panchromatic covering flat and mountain area of Lesotho. Results show that the projective transform model has equal or higher accuracy compared to the push-broom model. Conclusion is the projective transform model can be used in producing land use image map.

Key words Kingdom of Lesotho, BJ-1 small satellite, Geometric correction, Projection transformation model

1 Introduction

With the implementation of the second national land survey and national land use change survey and monitoring, China has formed a mature base map preparation technology for land use planning. To help other developing countries to learn this advanced technology, China Land Surveying and Planning Institute and the Department of Local Government and Chiefs of the Kingdom of Lesotho, successfully applied for " Lesotho Land Use Planning Technical Assistance Project" in April 2011, aimed at extending China's mature land use planning theories and methods and base map preparation technology for land use planning to Third World countries.

Land use remote sensing image is the important basis for the preparation of land use planning map. To have quick access to the image data fully covering the entire territory of the Kingdom of Lesotho, the project selects China's BJ-1 small satellite panchromatic image for the production of high-resolution land use remote sensing image. After the system geometric correction of the original panchromatic image, there is also a need to carry out geometric correction to reduce the geometric distortion of the image.

In general, the geometric correction model is an important factor affecting the accuracy of geometric correction. Existing literature has proposed a number of models, which can be roughly divided into the following two categories:

(i) Special sensor model. Mainly based on the geometric relationship of sensor imaging, it builds the strict geometric correction model of this sensor, such as linear push-broom model [1] and strict imaging model [2]. These models usually have high calibration accuracy, but they can be only used for the geometric correction of specified sensor.

(ii) General model. The general model is built mainly based on the geometric relationship of sensor imaging fitted by polynomial and other algebraic expressions, such as projection transformation model [3], rational function model [4], polynomial model [1], and finite element model [5]. Such model is not only versatile, but also has no need of the sensor parameters, so it is now widely used.

The terrain of the Kingdom of Lesotho is complex and we can not get a true reference image of the Kingdom of Lesotho, so there is a need to choose appropriate geometric correction model according to the characteristics and imaging principles of Beijing-1 panchromatic sensor.

2 Overview of BJ-1 satellite and geometric correction method

2.1 BJ-1 satellite Beijing-1 small satellite [6] is a small earth observation satellite with double panchromatic and multispectral sensors, jointly developed by China and the UK. It was launched on October 27, 2005. With three stabilized axes and design life of five years, it has a sun-synchronous orbit, and the orbital altitude is 686 km.

High-resolution panchromatic sensor is a linear CCD push-broom imager, and its imaging mode is shown in Fig. 1 [2]: the imaging mode of each line of image is the single central projection, and the imaging mode of the entire image is the multi-center projection.

2.2 Linear push-broom model The imaging principle of linear push-broom sensor [2] is that a line image is first formed on the surface, and then with the satellite's flight, sensor moves forward along a predetermined orbit, to obtain two-dimensional images by progressive push scanning.

Thus, each line in linear push-broom model can be expressed by the collinearity equation of central projection as shown in equation (1):

$$\begin{aligned} x_i = 0 = -f\frac{a_1(X_i - Xs_i) + b_1(Y_i - Ys_i) + c_1(Z_i - Zs_i)}{a_3(X_i - Xs_i) + b_3(Y_i - Ys_i) + c_3(Z_i - Zs_i)} \\ y_i = 0 = -f\frac{a_2(X_i - Xs_i) + b_2(Y_i - Ys_i) + c_2(Z_i - Zs_i)}{a_3(X_i - Xs_i) + b_3(Y_i - Ys_i) + c_3(Z_i - Zs_i)} \end{aligned} \quad (1)$$

where x is the flight direction; X_i, Y_i, and Z_i are the geographical

Received: January 24, 2014 Accepted: March 15, 2014
Supported by Application Demonstration System Project for High-resolution Remote Sensing of Land Resources (Stage I) (04 – Y30B01 – 9001 – 12/15).
* Corresponding author. E-mail: shunxiliu@163.com

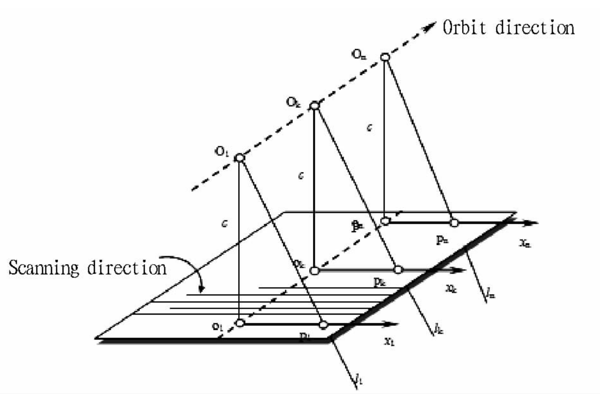

Fig. 1 Linear push-broom imaging mode

coordinates of the ground point i; x_i, y_i are the corresponding image coordinates; Xs_i, Ys_i, and Zs_i are the ground coordinates of imaging center; a_i, b_i, c_i are the function of exterior orientation elements of attitude angle of this line; f is the focal length of the sensor.

When carrying out the geometric processing of the remote sensing image acquired by the linear push-broom imaging sensor, it is generally assumed that the satellite motion is smooth and the three-axis attitude is balanced, so the polynomials can be used to describe the satellite's orbit and attitude, and by the polynomial model, the orbit and attitude data at any time are interpolated.

Normally, when using this model for geometric correction, it requires the focal length, pixel size, number of image pixels and other parameters of the known sensor. In the case of no satellite ephemeris parameters and no available sensor models, the linear push-broom model can not be used, but we can use the projection transformation model.

The projection transformation model can handle the geometric correction of multi-center projection satellite remote sensing image, so it can also be used for the geometric correction processing based on linear push-broom model.

2.3 Projection transformation model The essence of the projection transformation model is to use rational polynomial to simulate the geometrical relationship of the image in a flash of imaging, and associate the ground coordinates X, Y, Z with the corresponding image point coordinates x, y using rational polynomial.

Projection transformation model can be expressed as the formula (2):

$$Y=\frac{Num_L(X,Y,Z)}{Den_L(X,Y,Z)} \quad X=\frac{Num_S(X,Y,Z)}{Den_S(X,Y,Z)} \tag{2}$$

where $Num_L(X, Y, Z)$, $Den_L(X, Y, Z)$, $Num_S(X, Y, Z)$, $Den_S(X, Y, Z)$ and are the polynomial function of X, Y, Z (usually, degree of polynomial is 2 or 3).

According to the degree of image geometric distortion and geometric correction accuracy requirements, we can choose different degrees of polynomial. Denominator $Den_L(X, Y, Z)$ and $Den_S(X, Y, Z)$ can be equal or unequal. In different cases, the number of control points required is shown in Table 1.

The projection transformation model has been the linear polynomial form, so it does not need linearization, that is, a certain number of control points can be used to calculate rational polynomial coefficients, thereby carrying out geometric correction.

Table 1 The number of control points for solving the projection transformation model in different cases

Number	Same denominators	Different denominators
1	6	7
2	15	19
3	30	39

3 Experiment and analysis

Lesotho, officially the Kingdom of Lesotho, is a landlocked country completely surrounded by South Africa. It is just over 30000 km^2 in size. Lesotho covers 30355 km^2. It is the only independent state in the world that lies entirely above 1000 meters in elevation. Its lowest point of 1400 meters is thus the highest in the world. Over 80% of the country lies above 1800 meters.

Lesotho is also the southernmost landlocked country in the world and is entirely surrounded by South Africa. It lies between latitudes 28° and 31°S, and longitudes 27° and 30°E.

The real BJ-1 panchromatic image of two scenes Lesotho region is chosen for geometric correction experiment.

The first scene experimental image is the flat ground area image obtained on July 7, 2009, with the side look angel of −4.38° and elevation of about 1600 m. The ground object includes city buildings, roads, farmland, rivers, lakes, etc., as shown in Fig. 2-a.

The second scene experimental image is the high mountain area image obtained on August 15, 2009, with the side look angel of +4.88°. The ground object includes mountains, farmland, rivers, roads, etc., as shown in Fig. 2-b.

Since the true reference image of the Kingdom of Lesotho can not be obtained, Google Earth high resolution image (spatial resolution of about 0.5 − 1 m) is selected as the source of control point and check point, as shown in Fig. 2-c.

The elevation data is the digital elevation model (DEM) image with the interval of 30 m acquired by ASTER sensor, as shown in Fig. 2-d.

The experimental steps are as follows:

(i) Reprojecting the reference image and DEM image, to make the geographic coordinates meet WGS 84 coordinate system, UTM projection, 6 degrees zonation, Zone 35 (24 − 30E) projection zone.

(ii) Using the projection transformation geometric correction model provided by ERDAS 9.1 software, to set the regional minimum elevation at 0 m, and maximum elevation at 3476m.

(iii) Using the projection transformation model with the same denominator and 3rd-degree polynomial, the projection transformation model with the same denominator and 2nd-degree polynomial, and linear push-broom model provided by ERDAS LPS (modifying the sensor focal length to 1372 mm, CCD pixel size to 8 um, pixel number of image row to 6056, degree of orbit polynomial to 2, degree of polynomial of K attitude angle to 2, degree of polynomial of other attitude angles to 0) for experiment, respectively.

(iv) Selecting a certain number of control points and check points, to compare the residual error and root mean square error of the control points and check points with the same number and same distribution when using different geometric correction models. Experimental Image I selects 36 control points and 24 check points (distribution shown in Fig. 3-a), and Experimental Image II selects 43 control points and 29 check points (distribution shown in Fig. 3-b).

Table 2 is the residual error comparison figure of geometric correction control points and check points for Experimental Image I based on linear push-broom model, projection transformation model (2), and projection transformation model (3). It is found that:

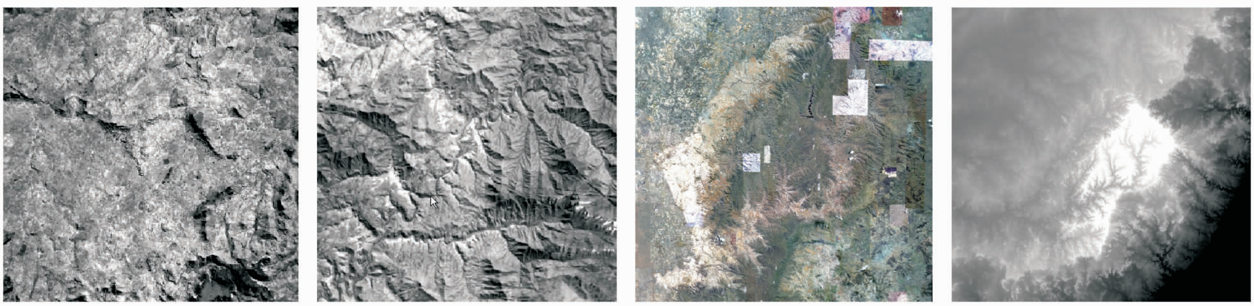

(a) Experimental Image I (b) Experimental Image II (c) Reference Image (d) DEM Image

Note: (a) Experimental Image I; (b) Experimental Image II; (c) Reference Image; (d) DEM Image.

Fig. 2 Data used for experiment

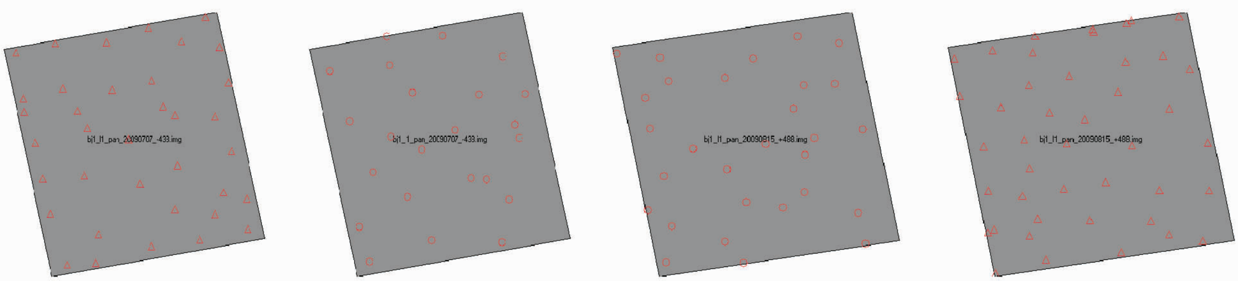

(a) Control points and check points for Experimental Image I (b) Control points and check points for Experimental Image II

Note: (a) Control points and check points for Experimental Image I; (b) Control points and check points for Experimental Image II.

Fig. 3 Distribution of control points and check points

(i) In terms of the residual error of control points, except the residual error of individual control points based on projection transformation model (2) greater than that based on linear push-broom model, the residual error of other control points for the two models is roughly equal; the residual error of projection transformation model (3) is 1 – 3 pixels less than that of the other two models.

(ii) In terms of the residual error of check points, it is basically consistent with the residual error of control points. The residual error based on linear push-broom model is roughly equal that based on projection transformation model (2); the residual error based on projection transformation model (2) is 1 – 2 pixels less than that based on linear push-broom model; the residual error of projection transformation model (3) is about 1 – 2 pixels less than that of the other two models.

Table 3 is the residual error comparison figure of geometric correction control points and check points for Experimental Image II based on linear push-broom model, projection transformation model (2), and projection transformation model (3).

It is found that the residual error of control points and check points based on linear push-broom model, projection transformation model (2) and projection transformation model (3) is roughly equal.

The root mean square error of control points and check points based on three models is shown in Table 4. In Experimental Image I, since the residual error of most control points and check points based on linear push-broom model and projection transformation model (2) is large, the root mean square error of the control points and check points is also large, about 4 pixels. Comparatively speaking, the root mean square error of control points and check points based on projection transformation model (3) is much less, about 2.5 pixels.

In Experimental Image II, the root mean square error of control points and check points in three models is roughly equal, about 6 pixels. By comparing the residual error in X direction and Y direction, it can be found that the residual error in Y direction is significantly less than that in X direction, which is due to the fact that in the push-broom imaging mode adopted by BJ-1 panchromatic sensor, X direction is the flight direction and Y direction is the single-center projection imaging.

Table 2 Residual error comparison of control points and check points for Experimental Image I

Model	Linear push-broom model	Projection transformation model (2)	Projection transformation model (3)
Residual error of control points	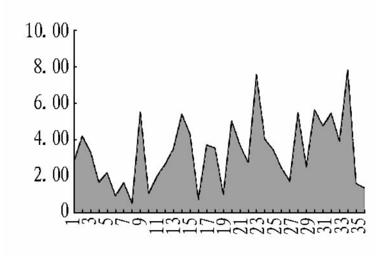	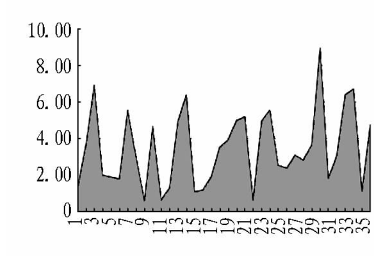	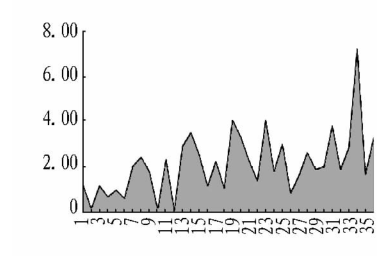
Residual error of check points	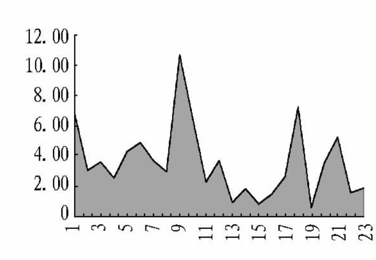	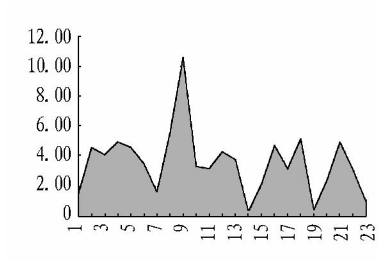	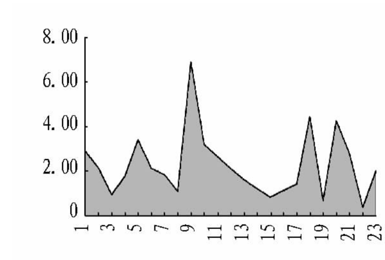

Table 3 Residual error comparison of control points and check points for Experimental Image II

Model	Linear push-broom model	Projection transformation model (2)	Projection transformation model (3)
Residual error of control points	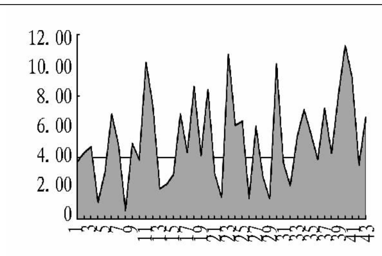	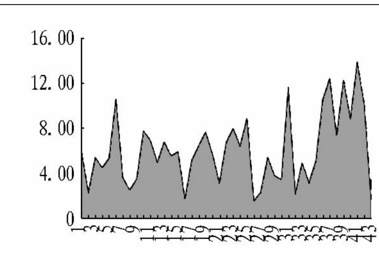	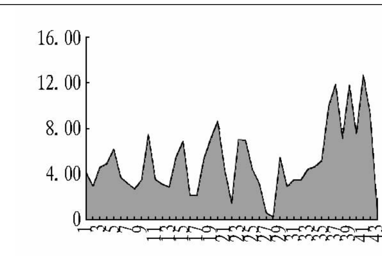
Residual error of check points	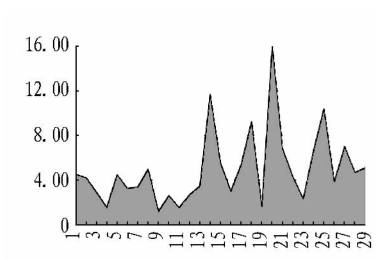	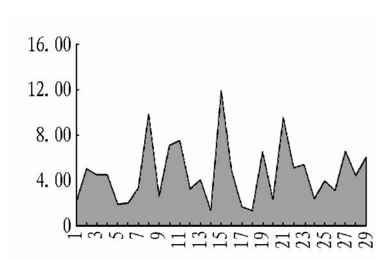	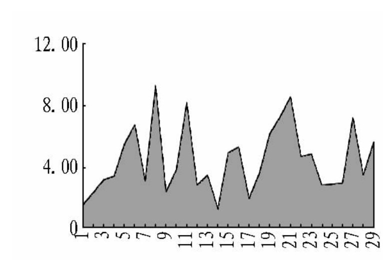

Table 4 Root mean square error comparison of control points and check points

Model	Type	Experimental Data I			Experimental Data II		
		X direction	Y direction	RMSE	X direction	Y direction	RMSE
Linear push-broom model	Control points	3.96	0.85	4.05	5.68	1.46	5.87
	Check points	3.87	1.60	4.19	5.67	1.75	5.94
Projection transformation model (2)	Control points	3.36	1.80	3.81	6.16	2.97	6.84
	Check points	3.64	2.34	4.33	4.53	2.82	5.34
Projection transformation model (3)	Control points	2.22	1.23	2.54	5.64	1.74	5.91
	Check points	2.27	1.42	2.68	4.07	2.71	4.89

4 Conclusions

By the real BJ-1 panchromatic image of Lesotho, the geometric correction accuracy based on linear push-broom model and projection transformation model is compared. The results show that in the flat ground areas, the geometric correction accuracy based on

(To page 84)

References

[1] IPCC. 2001: The IPCC data distribution center website[EB/OL]. http://www.ipcc-nggip.iges.or.jp/.

[2] SHI YF. The change trend of Chinese climate and sea level and its effect, vol.4, the effect of climatic change on water resources of northwest and North China[M]. Ji'nan: Shandong Science & Technology Press, 1995: 345-347. (in Chinese).

[3] QIU GY, WANG LM, HE XH, *et al*. Water use efficiency and evapotranspiration of winter wheat and its response to irrigation regime in the north China plane[J]. Agricultural and Forest Meteorology, 2008(93): 1-12.

[4] ZHANG XY, PEI D, HU CS. Conserving groundwater for irrigation in the North China Plain[J]. Irri. Sci, 2003(21): 159-166.

[5] ZHANG YQ, SHEN YJ, LIU CM, *et al*. Measurement and analysis of water, heat and CO_2 flux from a farmland in the North China Plain[J]. Acta Geographica Sinica, 2002, 57(3): 333-341. (in Chinese).

[6] Lascano RJ, Van Bavel CHM, Hatfield JL, *et al*. Energy and water balance of sparce crop: simulated and measured soil and crop evaporation[J]. Soil Sci. Soc. Am. J, 1987(51): 1113-1121.

[7] Van Bavel CHM, Lascano RJ. CONSERVN: a numerical method to compute soil water content and temperature profiles under a bare surface[D]. Remote Sensing Center, Texas, A & M University, College Station, TX, 1980, Technical report RCS-134.

[8] Van Bavel CHM, Lascano RJ, Stroosnijder L. Test and analysis of a model of water use by sorghum[J]. Soil Science, 1984(137): 443-456.

[9] Goudriaan J. Crop micrometeorology: a simulation study[R]. PUDOC, Wageningen, the Netherland, 1977.

[10] CHEN J. Mathematical analysis and simulation of crop micrometeorology [A]. Doctoral dissertation[C]. Department of theoretical production ecology, Agricultural University, Wagningen, the Netherland, 1984.

[11] Lascano RJ. Review of models for predicting soil water balance[A]. In soil water balance in the Sudan-sahelian zone[C]. (ed. By Sivakumar M.V.K., Wallace J.S., Renard C. and Giroux G.) Proc. Niamay workshop, Feb. 1991. IAHS Publ. no. 199. IAHS Press, Inst. of Hydrology, Wallingford, England: 443-458.

[12] Lascano RJ, Baumhardt RL, Hicks S K, *et al*. Soil and plant water evaporation from strip-tilled cotton: measurement and simulation[J]. Agron. J, 1994(86): 987-994.

[13] Lascano RJ, Baumhardt RL. Effect of crop residue on soil and plant water evaporation in a dryland cotton system[J]. Theor. Appl. Climatol, 1996 (54): 69-84.

[14] Krieg DR, Lascano RJ. Sorghum. In irrigation of agricultural crops[A] (ed. By Stewart B.A. and Nielsen D.) ASA, Madison, WI, 1990: 719-740.

[15] Steven RE, Terry AH, Arland DS. Energy and water balance for surface and subsurface drip irrigated corn. In Proceedings of the Fifth International Microirrigation Congress[A]. Orlando, FL. USA, 1995a: 135-140.

[16] Steven RE, Howell TA, Schneide AD, *et al*. Crop coefficient based evapotranspiration estimates compared with mechanistic model results[A]. In W.H. Espey and P.G. Combs (ed). Water Resources Engineering[C]. Vol.2. Proceedings of the First International Conference, San Antonio, Texas, Aug. 14-18, ASCE, New York, 1995b: 1585-1589.

[17] Qiu GY, Kazuro M, Tomohisa Y, *et al*. Separate estimation of evaporation and transpiration by ENWATBAL model[J]. J. Agric. Meteorol, 1998, 54 (3): 275-282.

[18] Qiu GY, Kazuro, Tomohisa Y, *et al*. Experimental verification of a mechanistic model to partition evapotranspiration into soil water and plant evaporation[J]. Agricultural and Forest Meteorology, 1999(93): 79-93.

[19] Qiu GY, Koichi M, Sadanori S, *et al*. Comparison of the three temperatures and conventional models for estimation of transpiration[J]. JARQ-Japan Agricultural Research Quarterly, 2002, 36(2): 73-82.

[20] Steven RE, Lascano RJ. ENWATBAL.BAS: a mechanistic evapotranspiration model written in compiled basic[J]. Agronomy Journal, 1993(85): 763-772.

[21] Willmott CJ. Some comments on the evaluation of model performance[J]. Bull Am. Meteorol. Soc, 1982, 63(11): 1309-1313.

[22] Durar A A, Steiner JL, Evett SR, *et al*. Measured and simulated surface soil drying[J]. Agron. J, 1995(87): 235-244.

[23] CHEN ZX, ZHENG GG, *et al*. Research on climatological problems during the sustainable development[M]. Beijing: China Meteorological Press, 2001: 106-144. (in Chinese).

[24] MIN JR, SU Y. Effect of climate warming on wheat production in China [A]. Research Group of the Effect of Climatic Change on Agriculture. The effect of climatic change on agriculture and the countermeasures[M]. Beijing: Peking University Press, 1992: 131-160. (in Chinese).

[25] LI CJ, LIU HB. Climate change in Shandong Province and its influence on potentiality of wheat production[J]. Meteorological Monthly, 2004, 30 (8): 49-53. (in Chinese).

[26] ZHOU L, WANG HJ, ZHU HW. Simulation study on the impact of climate warming on production of winter wheat in Huang-Huai-Hai Plain of China [J]. Journal of PLA University of Science and Technology, 2003, 4(2): 161-165. (in Chinese).

[27] HAO LS, MIN JZ, ZHANG WZ, *et al*. Impact of climate warming on winter wheat yield in Hebei Province[J]. Chinese Journal of Agrometeorology, 2009, 30(2): 204-207. (in Chinese).

[28] ZHANG JX, YAN JP. Evaluation model of wheat yield in regional response to climate change[J]. Journal of Arid Land Resources and Environment, 2003, 17(1): 85-90. (in Chinese).

(From page 78)

cubic polynomial projection transformation model can reach 2-3 pixels, and the geometric correction accuracy based on quadratic polynomial projection transformation model and quadratic polynomial linear push-broom model is about 4 pixels; in the high mountain areas, the geometric correction accuracy based on linear push-broom model and projection transformation model is roughly equal, about 6 pixels.

So, the cubic polynomial projection transformation model has the highest geometric correction accuracy, and it can be regarded as the geometric correction model for BJ-1 panchromatic image of the Kingdom of Lesotho. It should be noted that since we can not get more accurate geometric correction reference image of the Kingdom of Lesotho, this article uses Google Earth high-resolution image as the reference image for geometric correction, and geometric errors of its own will to a certain extent affect the geometric correction accuracy.

References

[1] SUN JB. Principles and applications of remote sensing[M]. Wuhan: Wuhan University Press, 2003. (in Chinese).

[2] ZHANG G. Rectification for high resolution remote sensing image under lack of ground control points [D]. Wuhan: Wuhan University, 2005. (in Chinese).

[3] FENG GY, LIU Y, LI JJ. Geometric rectification of aerial image-based camera projection model[J]. Modern Electronic Technique, 2007(23): 7-9. (in Chinese).

[4] Tao C.V., Hu Y. Investigation of the rational runction model[A]. Proceedings of ASPRS Annual Convention, 2000, Washington D.C. (on CDROM).

[5] WANG J, CHI YB, WANG Q, *et al*. Research on geometric correction method of China DMC remote sensing image[J]. Remote Sensing Information, 2006(6): 47-49. (in Chinese).

[6] CHEN ZC, LUO WF, ZHANG H, *et al*. The geometric evaluation of Beijing-1 microsatellite multispectral images[J]. Journal of Remote Sensing, 2006, 10(5): 690-692. (in Chinese).